



A novel and efficient epoxy/chitosan cement slurry for use in severe acidic environments of oil wells—Structural characterization and kinetic modeling

Antonio R. Cestari*, Eunice F.S. Vieira, Fernanda J. Alves, Ellen C.S. Silva, Marcos A.S. Andrade Jr.

Laboratory of Materials and Calorimetry, Department of Chemistry/CCET, University Federal of Sergipe, 49100-000, São Cristóvão, Sergipe, Brazil

ARTICLE INFO

Article history:

Received 10 October 2011

Received in revised form 6 January 2012

Accepted 20 January 2012

Available online 27 January 2012

Keywords:

Oil well cement slurries

Epoxy resins

Chitosan

Kinetics

Environmental-friendly materials

ABSTRACT

In this study, the biopolymer chitosan was used to synthesize a new epoxy/chitosan cement slurry. The features of the new slurry were evaluated in relation to a standard cement slurry ($w/c=0.5$). A kinetic study of the interaction epoxy/chitosan slurry/HCl was performed to simulate the use of the new slurry in environmental-friendly acidizing procedures of oil wells. The experimental data were well fitted to a three-parameter kinetic model. The analysis of the kinetic modeling suggests that surface reactions constitute the main interactions at the interface epoxy/chitosan-modified cement slurry/HCl. The characterization of the slurries was performed by FTIR, XRD, TG/DTG and solid-state reflectance spectroscopy. The results have pointed out that the main features of the new cement slurry were preserved, even after long-term contact with HCl in aqueous solution. The results of this study underline the excellent features of the new epoxy/chitosan-modified cement slurry for using in environmental-friendly acidizing procedures of oil wells.

© 2012 Elsevier B.V. All rights reserved.

1. Introduction

The oil and gas industry has worked for a long time to meet the challenge of providing environmental protection. However, the exploitation of oil and gas reserves has not always been without some ecological side effects. Anyway, the environmental impacts may be avoided, minimized or mitigated.

Cementing is an essential operation during construction of an oil or gas well [1]. Oil well cementing is the process of placing cement slurry in the annulus space between the well casing and the geological formations surrounding to the well bore, from the injection horizon to the surface. This procedure is used for providing zonal isolation of different subterranean formations in order to prevent exchange of gas or fluids among different geological formations, as well as for protecting oil producing zones from corrosion and collapse. Oil well cementing is less tolerant to errors than conventional cementing works and long-term performance of the oil well cement slurries is of great concern [2]. If the cement does not provide a good seal, gas or liquid fluids can migrate to the surface and lead to explosions or environmental problems [1]. So, the main environmental-friendly aspect in oil and gas industry focuses not only on the prevention of destruction of oil well cement packs, but also on the increasing of their chemical integrities.

One such method commonly employed in oil and gas industry is known as acidizing stimulation of oil wells [3]. In usual well-acidizing procedures, a non-oxidizing mineral acid is introduced into the well and is forced into the adjacent subterranean formation where it reacts with acid-reactive components, such as calcium carbonate, magnesium carbonate, and others. The usual acid employed in such acidizing procedures is hydrochloric acid. However, several oil wells have been observed to exhibit well zonal intercommunication problems due to problems in the cement slurries. It is due to reactions between common hardened slurries in the annulus and the acidic solution. As a consequence, acid (even oil) spill may cause long-term environmental problems [3,4]. So, stability of oil well cement slurries is of great concern in order to avoid environmental impacts. In this way, cementing of deep wells requires new materials that provide protection against reactions in acidic media. The protective characteristics of oil well cements may be controlled by the addition of polymeric additives [5].

The use of specific polymeric nets has been highly effective in preventing destruction and increasing the internal cohesion of oil well cement packs. The literature data have been proved the ability of epoxy resins to improve the chemical properties of cement slurries when compared with conventional cement slurries [6]. Epoxy resins are useful to promote physico-chemical interactions and ensure excellent levels of adhesion between the mineral and organic phases of polymer-modified cement slurries [5,6].

Epoxy cement mortars are composed of cured epoxy resin, cement and fine aggregates. Epoxy resin systems are made up of an epoxy resin and a curing agent (also called a hardener or catalyst).

* Corresponding author. Tel.: +55 79 21056656; fax: +55 79 21056684.
E-mail address: cestari@ufs.br (A.R. Cestari).

Common epoxy formulations are based on diglycidyl ether of bisphenol A resins that can be crosslinked with a wide variety of hardeners such as amines, organic acids, anhydrides and others [7]. In most cases, the epoxy cement mortars with hardeners have properties that are better than the mortars without a hardener [8]. In addition, the polymeric nets of epoxy resins are typically insoluble in the aqueous mineral acid solutions employed in acidizing operations of oil wells. However, each component of the epoxy resin can be hazardous [9,10].

The chemicals in epoxy resin systems can affect human health when they come in contact with skin, or if they evaporate or form a mist or dust in the air. Diluents and solvents are often used to dilute or thin epoxy resins, which are usually toxic liquids with strong, unpleasant odors. Some studies suggest that they may be cancer-causing agents and cause birth defects in test animals [11]. On the other hand, it was found that cyclic amines or polyamides are generally less hazardous than aliphatic amines [11]. In this work, it is intended to use the amphiphilic biopolymer chitosan as a hardener in a new epoxy-cement system for use in environmental-friendly oil well operations in order to minimize health effects of traditional epoxy resin chemicals.

Chitosan, the deacetylated derivative of chitin, is the second most abundant natural polysaccharide. As chitosan bears amine and alcohol functions, it may react with epoxy resins by polyaddition reactions [12]. However, as far as we know, almost nothing is known about the role of the presence of the epoxy/chitosan polymeric net in oil well cement systems. Some aspects concerning the main features of the new epoxy/chitosan-cement slurry, before and after interaction of pH 1.0 HCl solution, are presented and discussed.

2. Experimental

2.1. Materials and reagents

Water was used after double-distillation. Powder cement (200–325 mesh, Class A special for oil well cementation) from Cimesa Special Cements (Laranjeiras, Brazil) was used. Silica gel of 150–300 mesh (particles diameter), from Schumberger Petroleum Services (Nossa Senhora do Socorro/SE, Brazil), was used in the slurries preparations. The epoxy resin (diglycidyl ether of bisphenol A) was supplied by The Huntsman Co Special Resins. The chitosan powder was a free gift from C.E. Roeper GmbH, Hamburg (Germany). The following characterizations were performed and described earlier [13], in order to check some important aspects concerning the purity and structural aspects of the chitosan sample. Briefly, the degree of deacetylation (82%) was determined by FTIR. Solid-state ^{13}C NMR spectroscopy was used to verify the purity of the chitosan sample. The quantity of nitrogen ($8.26 \pm 0.33\%$) was determined by the Kjeldhal method. The idealized chemical structures of the epoxy resin and chitosan are shown in Fig. 1.

2.2. Preparation of the cement slurries

The mixing procedure adopted was in accordance with the American Petroleum Institute (API) practice was described earlier [14]. It was consisted of mixing the cement, epoxy resin, chitosan and water for 30 s at 12,000 rpm [11,12]. The amounts of the components of the slurries were calculated in relation to a final density of the cured slurries from 1.50 to 2.00 g cm^{-3} [10–12]. In order to avoid uncompleted polymerization, the proportion of epoxy resin/chitosan was 1:2. The cement, silica and water were used to obtain the standard cement slurry ($w/c = 0.5$) for comparative purposes. The cement slurries were cast into cubic molds with 5.08 cm sides and cured in water for 28 days before use. For simplicity,

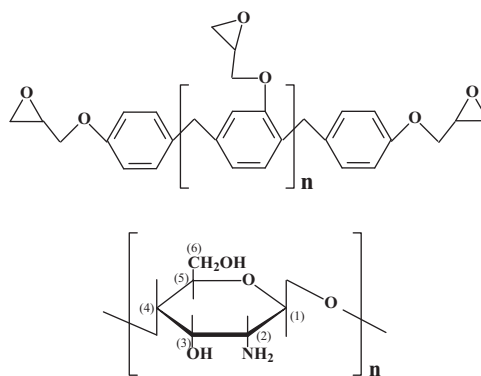


Fig. 1. Idealized chemical structures of the epoxy resin (above) and chitosan (below).

the slurries are hereafter denominated as Chit/epoxy-slurry (cement, water, silica, epoxy resin and chitosan) and standard-slurry (cement, silica and water).

2.3. Kinetic experiments of HCl interaction with the cement slurries

The experiments were performed using a temperature-controlled water bath, from 25 to $55 \pm 0.1^\circ\text{C}$. In a typical experiment, a cubic cemented sample was put in contact with 400 mL of 0.10 mol L^{-1} HCl solution in a sealed glass container at a determined temperature. At predetermined times, the HCl concentrations in the solutions were determined using a pH meter. All determinations were carried out in triplicate runs. The amounts of acid adsorbed were calculated using Eq. (1) [15]:

$$q_t = \frac{(C_i - C_t)V}{m} \quad (1)$$

where q_t is the fixed quantity of acidic species per gram of slurry at a given time t in mol g^{-1} , C_i is the initial concentration of acidic species in mol L^{-1} , C_t is the concentration of acidic species at a given time t in mol L^{-1} , V is the volume of the solution in L and m is the mass of slurry in g.

2.4. Characterization of the cement slurries

The thermogravimetric analyses (TG and DTG) were made using about 10 mg of material, under synthetic air atmosphere from 25 to 800°C , in a SDT 2960 thermoanalyzer, from TA Instruments. DRX-ray analyses were performed in a Shimadzu diffractometer, in the 2θ range from 5° to 60° (accumulation rate of $0.02^\circ \text{ min}^{-1}$), using Cu $K\alpha$ radiation. Infrared spectral data were obtained on a Perkin Elmer 1600 series FTIR spectrophotometer at a resolution of 4.0 cm^{-1} . The solid-state reflectance spectra of the samples were recorded on an Ocean Optics UV-Vis spectrophotometer from 400 to 900 cm^{-1} at a resolution of 4.0 cm^{-1} .

According to the results of the kinetic study, the cement samples with maximum amount of HCl adsorbed (after 40 h of contact time) were also chosen for characterization.

3. Results and discussion

3.1. Some considerations on cement chemistry, chitosan and epoxy resins

Cured cements have complex internal microstructures with different clinker phases hydrated at different rates. The composition of oil well cement slurries are usually based upon four principal mineral phases [1]: tricalcium silicate (Ca_3SiO_5 , or C_3S), dicalcium

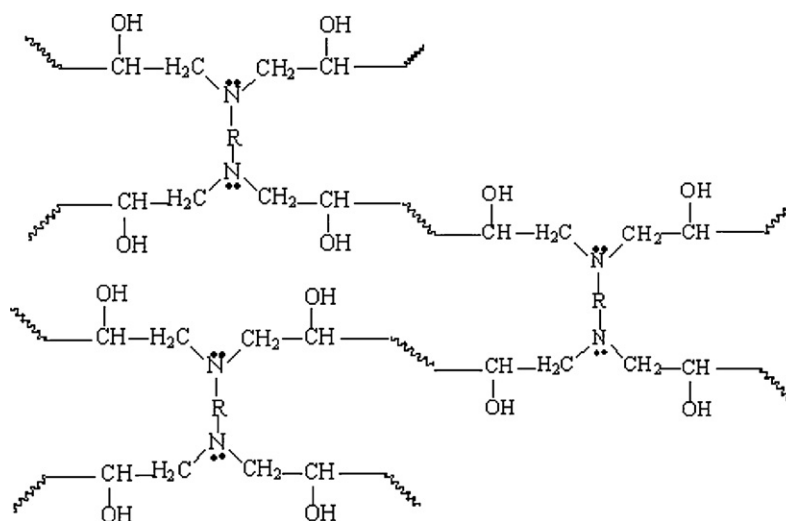


Fig. 2. Idealized structure of polymerized amine-cross-linked epoxy resins.

silicate (Ca_2SiO_4 , or C_2S), tricalcium aluminate ($\text{Ca}_3\text{Al}_2\text{O}_6$, or C_3A), calcium aluminoferrite (C_4AF) of variable composition. These mineral phases are intimately mixed in the form of cement grains.

The calcium silicate hydrate system formed (C-S-H), is typically a poorly crystalline non-stoichiometric material consisting principally of mixings of dimeric units at first, but which subsequently slowly polymerizes after a few days. In addition, portlandite ($\text{Ca}(\text{OH})_2$) is also formed in the hydration system [1]. However, the portlandite released during cement hydration is partially consumed as a result of interaction with active silica fume. In general, sulphate is added to all cements in the form of calcium sulphate. If not, the C_3A and C_4AF phases may quickly hydrate and cause flash set (loss of workability) [16].

The most rapid reaction during the early hours of cement hydration at ambient temperature is due to the formation of ettringite, a hydrous calcium aluminum sulfate mineral ($\text{Ca}_6\text{Al}_2(\text{SO}_4)_3(\text{OH})_{12} \cdot 26\text{H}_2\text{O}$). At the beginning of hydration the aqueous phase of the cement slurry can be considered for simplicity as essentially a limewater medium, being derived from hydration as follows [17]:



One of the most common additives in cement admixture in oil field industry is silica flour, which is typically a pozzolanic material in nature [18]. Silica is also considered as a lightener agent due to the fineness of the particles and is added to prevent strength degradation of the cement slurry by forming specific crystalline C-S-H hydrates. The tiny particles of silica place in pores in micron size lead to porosity and permeability reduction. Literature data have demonstrated that the inclusion of silica reduces the setting time and increases the strength (compressive, tensile) of cement slurries [18].

The presence of water-soluble polymers in cement mortars influences the rate and degree of cement hydration, as well as the nature and amount of hydration products that are formed. The microstructures of the hydrate crystals are also changed. This is due to partial intercalation of the polymer chains within the cement hydrate lattice [19]. The mechanism by which polymers act is not well understood and is still a matter of controversy, but it is known that they are able to partially inhibit the growth of ettringite and portlandite crystals. During hardening, two processes can take place, i.e. cement hydration and polymer film formation. In general, organic polymeric additives have shown to strongly interact

with the surface of hydrated C-S-H , controlling the pathways of the interaction between the organic molecules [20].

Cement mortars modified with water-soluble polymers show higher water retention than ordinary cement mortars. The hydrophilic parts of the polymers interact with the water molecules in the fresh mixture, preventing the dry-out by evaporation and absorption into the surrounding porous material [1]. The water retaining capacity also often results in a thickening and viscosity enhancing behavior. Because of the increased viscosity of the cement paste, less free water is available for bleeding and the segregation tendency decreases. So, the homogeneity of the mortar is improved.

Chitosan is a derivative of chitin by removing most of the acetyl groups of chitin using strong alkalis. Chitosan has highly sophisticated functionality and a wide range of applications in several industrial areas [12,21]. The degree of crystallinity of chitosan is a function of its degree of deacetylation. In general, in order to obtain a soluble product the degree of deacetylation of chitosan must be higher than 80%. The attached side groups on chitosan provide versatile materials with specific properties. The active primary amino groups on the molecule provide sites for a variety of attachments employing mild reaction conditions [12,21].

The epoxy-amine system cure progressively transforms an initially fluid small-molecule mixture into an insoluble network, which is typically solid [11]. However, the chemistry involved in the epoxy/chitosan curing process is rather complex and still not completely understood. An Idealized structure of polymerized amine-crosslinked epoxy resins is shown in Fig. 2. In fact, there are several reactions participating in the formation of the epoxy/amine hardener network. Competitive chemical reactions accompanied by complex physical phenomena occur during curing, when the system passes from a mixture of linear and branched oligo- and polymers into a single, three-dimensional, macromolecule [22]. In general, at least four reactions of epoxy cure with primary amine groups of chitosan can occur. The first reaction is between an epoxide ring and a primary amine to produce a secondary amine and a hydroxyl group. The formed secondary amine can also react with an epoxide to produce a tertiary amine and a new hydroxyl group. Another possible reaction is the etherification between a hydroxyl group of secondary amine and an epoxide to form an ether link and a new hydroxyl group. In general, the primary amine sites in this system act as chain extenders while the secondary amines produce branched and crosslinked structures.

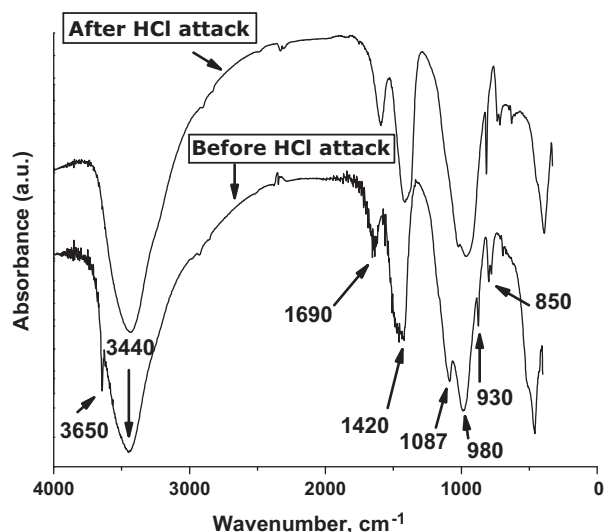


Fig. 3. FTIR curves of standard slurry before and after HCl interaction.

3.2. Characterization of the materials

Characterization features can provide useful information about microstructural changes in the cement slurries synthesized in this work. Figs. 3 and 4 show the FTIR spectra of the standard slurry and Chit/epoxy-slurry, both before and after HCl interaction. The main information is related to silicate polymerization, presences of portlandite and TO_4 condensed tetrahedra in cement chains with T= Si or Al (Si–O–Si or Al–O–Si bonds), possible identification of calcium carbonate polymorphs, and physically adsorbed water [23]. However, interpretation of the OH-stretching region in the mid-IR spectra ($2800\text{--}4000\text{ cm}^{-1}$) is difficult because bands are broad and overlap.

For the standard slurry, the small narrow band at 3650 cm^{-1} is due to Ca–OH vibrations from portlandite. The broad bands centered at 3440 and 1690 cm^{-1} are due to stretching vibrations of O–H groups in H_2O or hydroxyls of hydrated products with a wide range of hydrogen bond strengths [24]. The band centered at around 1085 cm^{-1} is assigned to Si–O stretching vibrations of the SiO_4 tetrahedral units, characteristic of a silica-rich material or the

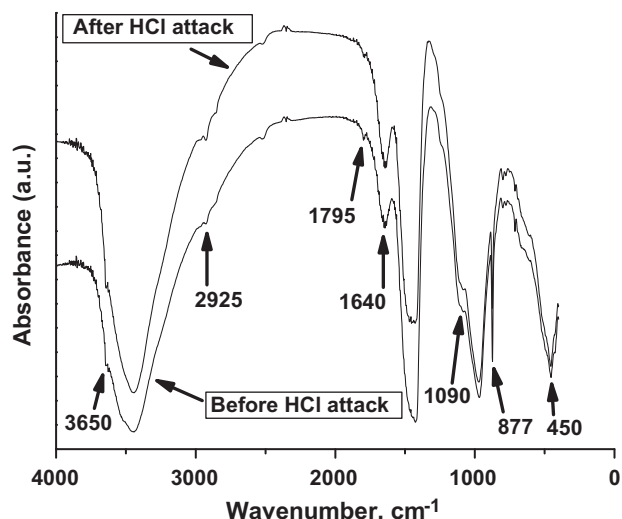


Fig. 4. FTIR curves of the Chit/epoxy-slurry before and after HCl interaction.

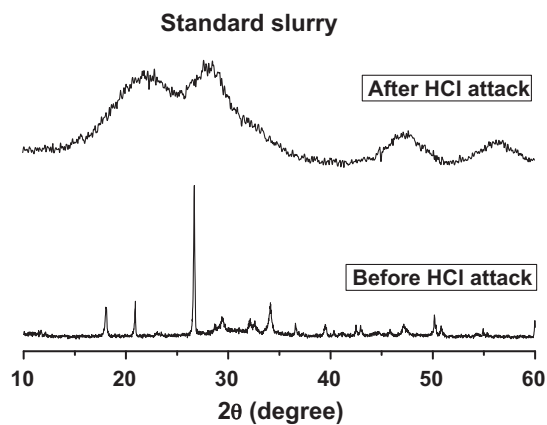


Fig. 5. DRX diffractogram of the standard slurry before and after HCl interaction.

presence of C–S–H mixes [23]. Condensation reactions involving Si–OH and Al–OH groups, i.e. Si–O–Al or aluminosilicate bonds can also occur. However, the Si–O stretching bands usually overlap the ettringite bands at around 1000 cm^{-1} and 1120 cm^{-1} . The band appearing at 460 cm^{-1} is associated with O–Si–O bending vibrations, which is influenced by O–Si–O angle and presence of neighboring sites. The characteristic bands of calcium carbonate can theoretically be found at 1420 and 850 cm^{-1} . Because of their different crystal structure the three polymorphs of calcium carbonate (calcite, vaterite, and aragonite) can be discriminated using FTIR. In this way, the small bands centered at 850 and 1460 cm^{-1} suggest the presence of aragonite [23].

The mid-IR bands change systematically in frequency and/or intensity with, which are related with silicate reaction after HCl interaction [23]. It can be observed disappearance of the peaks at 3650 and 1087 cm^{-1} , suggesting, respectively, partial leaching of portlandite and progressive depolymerization of silicates chains with possible formation of new aluminosilicates [25].

The identification of polymers within the cementitious matrix is a major problem, due to the low polymer amounts in the cement samples. Anyway, looking at the FTIR curves of the chemically modified cement materials, it is supposed that the formation of epoxy/chitosan polymeric net causes a reorganization of microstructure. The presence of bands at 2925 and 1795 cm^{-1} are due to the presence of both alkyl ($-\text{CH}_3$, $-\text{CH}_2$) and ester ($-\text{C}(\text{O})-\text{O}$) groups of the epoxy resin, respectively. The presence of the epoxy resin/chitosan polymeric net is also proven by the presence of the absorption band at 877 cm^{-1} associated with the C–H stretching vibration of the epoxide group. In addition, the sharp peak at 3650 cm^{-1} is attenuated and only a shoulder appears which may corresponds to hydrogen bonding between the cement phases and the epoxy-chitosan polymeric net [26]. It may be considered as an evidence of the partial inhibitive effect of the epoxy-chitosan resin on the formation of portlandite during the hydration of the Chit/epoxy-slurry. In general, the FTIR spectrum of Chit/epoxy-slurry after exposure to HCl solution is more or less the same in relation to the raw Chit/epoxy-slurry. It seems to be a clear indication of the protective effect of the epoxy-chitosan resin against the leaching out the chemical components of the chitosan/epoxy-modified cement slurry in the presence of HCl.

The XDR profiles of the slurries are presented in Figs. 5 and 6. The potential uses of XRD powder diffraction in the study of cured cement materials are related to determination of phase composition, determination of polymorphic modifications and state of crystallinity of individual phases. However, difficulties in quantitative analysis are caused by variability of patterns of phases due to compositional or polymorphic variation, and for the ferrite phase,

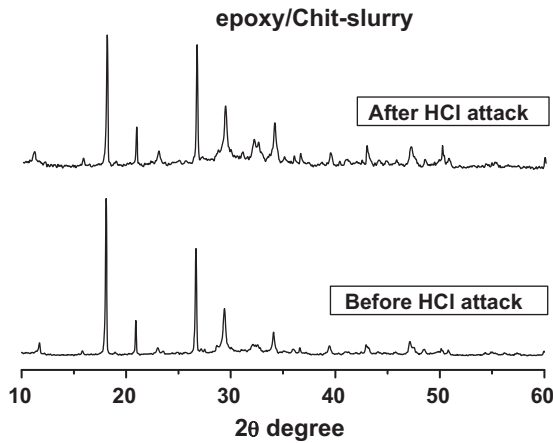


Fig. 6. DRX diffractogram of the Chit/epoxy-slurry before and after HCl interaction.

peak broadening or imperfect crystallinity. Moreover, the symmetry of the solid solutions changes, which affects X-ray intensities. In addition, XRD reflections from different minerals coincide or overlap [27].

For the standard slurry, the main products are portlandite, ettringite and ill crystallized C–S–H ($2\theta = 25^\circ\text{--}35^\circ$) [27]. C_3S is normally so much the predominant phase that its pattern tends to swamp those of the other phases. In general, the stronger peaks of C_2S are overlapped by ones of C_3S . It is suggested the presence of major products of portlandite ($2\theta = 18^\circ$), calcite and C_3S ($2\theta = 27^\circ$), ettringite ($2\theta = 34^\circ$), a mixture of C_2S and portlandite, and tobermorite [$Ca_5Si_5Al(OH)O_{17}\cdot 5H_2O$] (a strength retrogression inhibitor presents in cured oil well slurries [1]) ($2\theta = 47^\circ$) [28], and mixtures of quartz, calcite and aragonite ($2\theta = 21^\circ$ and 28°) [29]. For the epoxy/Chit slurry, a relatively similar XRD profile was observed.

Some features of the microstructure of the slurries have changed after HCl interaction. From observation of the standard slurry XRD diffractogram, the crystalline aspect of this cement slurry decreased markedly. So, XRD does not allow the determination of the slurries constituents after HCl interaction properly. On the other hand, the XRD diffractogram of epoxy/Chit slurry after HCl interaction is more or less the same in relation to this same material before HCl interaction. It also seems to be clearly evidenced that the structure of the epoxy/Chit slurry remains its main morphological characteristics, even after HCl interaction.

The plots of TG/DTG are shown in Figs. 7 and 8. Thermal analysis (TG/DTG) can be used to determine quantitatively from the mass loss of the liquid (typically H_2O), gas (typically CO_2), as well as to further analyze some cement phases which do not appear by the use of XRD technique which only shows the crystalline phases. However, the identification of mineral components and their quantification using TG/DTG is not easy due to overlapping processes [30].

Upon heating, cement slurries have shown a continuous sequence of more or less irreversible decomposition reactions. The results from TG for the standard slurry before HCl interaction have shown five main mass loss transitions: the release of evaporable adsorbed water ($\approx 30\text{--}120^\circ\text{C}$), the decomposition of gypsum and ettringite, the loss of water from partial decomposition of carboaluminate hydrates ($\approx 120\text{--}190^\circ\text{C}$), the loss of bound water from the decomposition of C–S–H and carboaluminate hydrates ($\approx 190\text{--}420^\circ\text{C}$), the loss of water from portlandite dehydration ($\approx 420\text{--}475^\circ\text{C}$), and the decomposition of carbonate phases, typically calcium carbonate ($\approx 475\text{--}700^\circ\text{C}$) [31].

A very small peak at about 170°C is due to the dehydration of C–S–H and formation of monocarboaluminates. This peak is very difficult to see as it is just a slightly change of slope of the

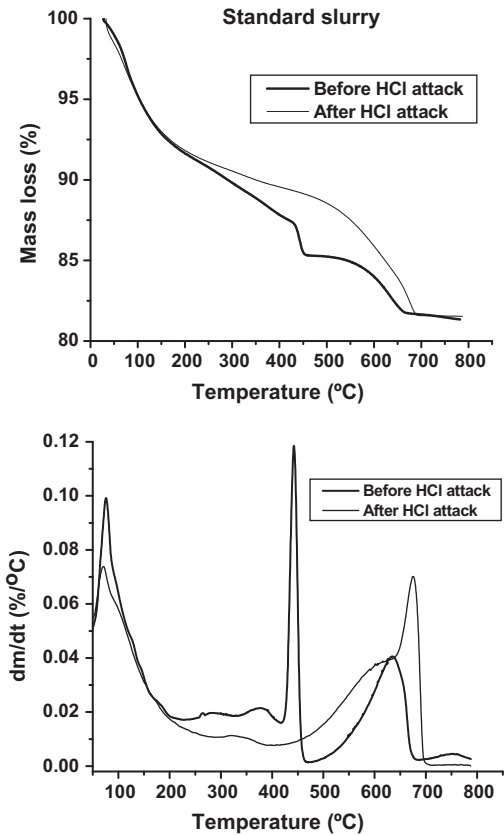


Fig. 7. TG (above) and DTG (below) curves of the standard slurry before and after HCl interaction.

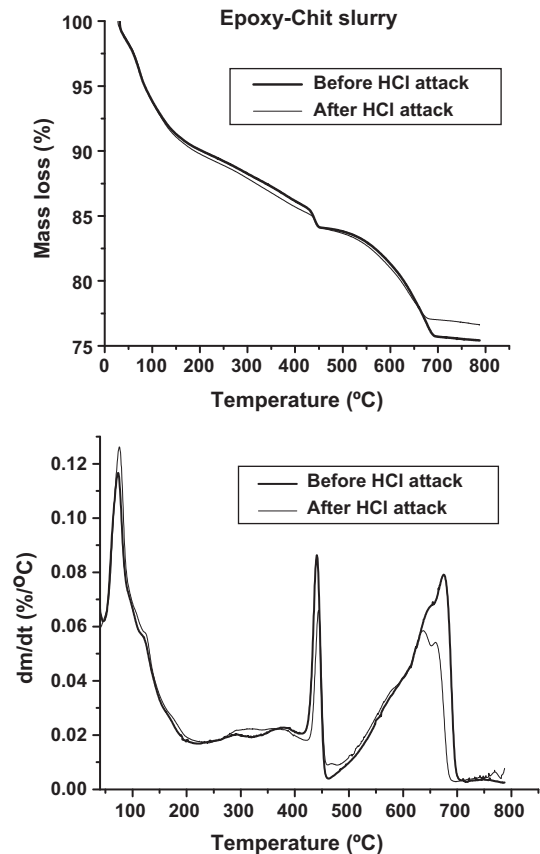


Fig. 8. TG (above) and DTG (below) curves of the Chit/epoxy-slurry before and after HCl interaction.

TG curve [31,32]. The thermal dehydration of C–S–H phases can be considered as irreversible reactions [32]. Ettringite decomposes to give monoaluminosulfates, which are themselves unstable at higher temperatures and are typically converted to a stable, crystalline hydrogarnet phase. After heating at 70 °C, the short-range order of ettringite is disrupted, and becomes amorphous in nature. Thereafter, the rest of the H₂O molecules in the Ca polyhedra are removed, and the ettringite microstructure is destroyed. This step is typically accompanied by changes in the coordination number of Al from 6 to 4 [33]. The TG/DTG curves of Chit/epoxy-slurry after exposure to HCl solution is more or less the same in relation to the Chit/epoxy-slurry before HCl interaction.

From TG/DTG curves, the portlandite content was determined using Eq. (3) [34]:

$$CH (\%) = \frac{\Delta_{CH} (\%) \times M_{CH}}{M_w} \quad (3)$$

where CH (%) is the content of portlandite, $\Delta_{CH} (\%)$ is the weight loss during the dehydration of calcium hydroxide, M_{CH} is the molar weight of calcium hydroxide and M_w is the molar mass of water.

For the standard slurry and Chit/epoxy-slurry, the content of portlandite was found to be 7.64, and 6.13%, respectively. After HCl interaction, for the standard slurry, it can be clearly observed that the weight loss related to the dehydroxylation of portlandite is undetectable. However, for Chit/epoxy-slurry, the portlandite content only slightly decreased to 4.00%.

It has been shown that the presence of organic polymers can significantly influence the morphology of portlandite in cement matrices, depending on the type of polymer, the brand of polymer, the polymer-cement ratio or a combination of all these factors. Portlandite crystals represent the weak phase in the cement matrix and the surfaces of those crystals form preferred cleavage sites [35]. It has been postulated that the polymer particles act as a kind of a bonding agent between the different layers, increasing the interparticle bonding. By “gluing” the crystal layers together, the microstructure of the cement slurry is strengthened [35].

These all conclusions from TG/DTG curves seem to be very consistent with results from FTIR and DRX characterization.

In this work, solid-state diffuse reflectance (DR) is used to complement the morphological studies of the cement slurries, because DR is sensitive to changes in chemical environments of solid samples. The DR spectra of the slurries are shown in Fig. 9. The DR spectrum of the standard slurry shows a broad absorption band at the visible wavelengths with a maximum absorption at about 580 nm. After HCl interaction, this broad band is shifted to about 620 nm. These two absorption bands have been considered to be associated with crystal field absorptions of Fe(III) in octahedral coordination with oxygen in hematite (580 nm) and ferrihydrite (620 nm) [36]. On the other hand, the analysis of the spectra has not suggested changes in the DR spectra of Chit/epoxy-slurry after HCl interaction. This suggests that the interaction with HCl was too little to affect the coordination of the central metal ions of hematite in type of cement slurry. However, the attribution of DR peaks is open to speculation. Band overlapping and poor spectral resolutions have generally precluded details of the chemical environment of Fe oxides in cement systems by DR [37].

In fact, trace metals associate with Fe(III) oxides can be found in cemented bodies [38]. Fe(III) oxides with discrete amorphous or crystalline phases are typically high in surface area, form particle coatings of complex and varied composition, and are reactive [37]. Ferrihydrite is known to contain 6-fold coordinated ferric ions. In alkaline conditions, it possesses a goethite/akaganeite-like local structure around Fe. However, we are unable to discuss the transformation of hematite to ferrihydrite in the presence of HCl, using the experimental results of this work. In addition, this specific aspect is assumed to be beyond the scope of this work.

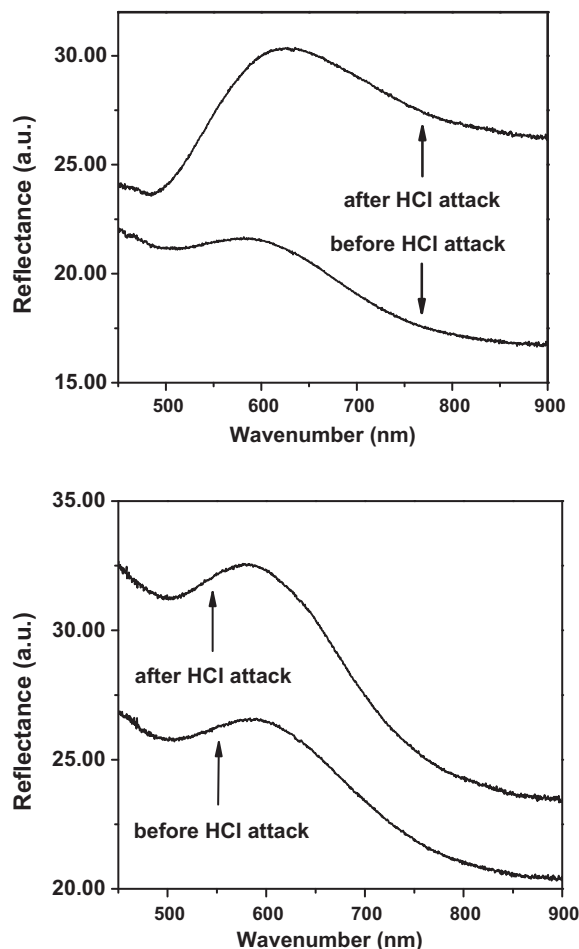


Fig. 9. Diffuse reflectance spectra of the slurries before and after HCl interaction.

The characterization results have pointed out similarities between the cement slurry with the presence of the epoxy/chitosan polymeric net, before and after HCl interaction. It underlines the exceptional stability of this new type of cement slurry in the presence of acidic species in solution.

3.3. Kinetic modeling of HCl interaction on the cement slurries

The rate of corrosion of cement slurries in acidic medium is related to the type of cement composition, the concentration of the acid and the acid strength. Hydrochloric acid is very aggressive due to both its dissociation ability and high solubility of its calcium salts [38,39]. In general, the dissolution of ferrite or aluminates hydrates and the corresponding loss of Fe(III) and Al(III) are slow and occur at low pH [39]. An important task for determining kinetic parameters is to quantify the acid interaction as a function of contact time.

Fig. 10 shows the HCl interaction amounts on Chit/epoxy-slurry, which is progressively occupied by the acid. The amount of HCl adsorbed increases with contact time and it remains constant after an equilibrium contact time in relation to temperature. It is also noted that the amount of sorbed HCl on Chit/epoxy-slurry increased from 25 to 55 °C. It is worth to be mentioned that interaction of HCl with the standard slurry was not described in this work, because the experimental results using this slurry were irreproducible and difficult to analyze, due probably to its chemical degradation in the presence of HCl, as shown in the characterization section of this work.

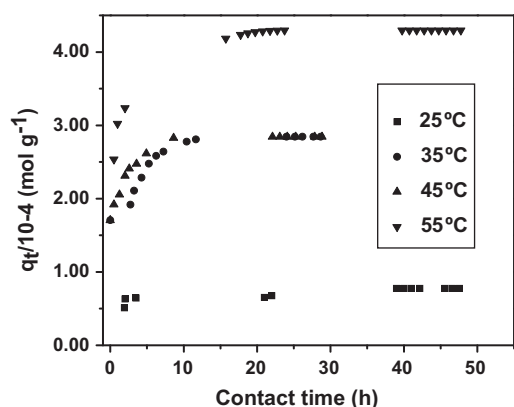


Fig. 10. Interaction profiles of HCl on the Chit/epoxy-slurry in relation to the contact time, at different temperatures. Initial [HCl] = 0.10 mol L⁻¹.

Interaction mechanisms at solid/solution interfaces may vary with temperature [40]. In general, with the increase of temperature external mass transport begins to play an important role in HCl interaction by Chit/epoxy-slurry. Generally speaking, interactions at solid/solution interfaces increases with temperature because high temperatures provide a faster rate of diffusion of adsorbate species from the solution to the solid surface. At low temperatures, HCl interaction is limited by the external mass transport and the interaction rate constant (k) is slightly lower in relation to the interaction rate constants at high temperatures. When temperature increases, the thickness of the boundary layer surrounding the sorbent (slurry) decreases and the mass transport resistance of the acidic species in solution increases [1]. Thus, the diffusion rate of the adsorbate in solution (HCl in the present study) in the external mass transport process increases with temperature.

Predicting the rate at which solid/solution interactions take place in a given solid/solution system is one of the most crucial factors for the effective analysis. The development of an appropriate model can be based on accepting a certain fundamental approach to interfacial kinetics and its further modification in order to adopt it for a given solid/solution system. The kinetic parameters may vary with temperature, and the amount of acid in solid phase and the rate constants in a given kinetic model may not be invariable [41]. The HCl interaction should be visualized using a Avrami-like three-adjustable-parameter exponential function, as shown in Eq. (4) [15]:

$$q_t = q_e(1 - \exp^{-[k \cdot t]^n}) \quad (4)$$

where q_t and q_e denote the amount of HCl at given time t and at equilibrium, respectively; k is the rate constant and n is another constant, which is related to changes of HCl interaction mechanism. A nonlinear methodology was used for calculating and analyzing the kinetic parameters. The experimental and calculated comparative values of the adsorption amounts (q_t) in relation to the exponential kinetic model are shown in Table 1. In this work, in

Table 1

Values of the parameters of the three-parameter kinetic model and Chi-square coefficients of HCl interaction on the epoxy/chitosan cement slurry as a function of temperature.

Temp. (°C)	n	k (h ⁻¹)	$Q_e/10^{-4}$ (mol g ⁻¹)	χ^2
25	1.28	0.067	0.80	7.74×10^{-11}
35	0.48	0.393	4.30	2.10×10^{-11}
45	0.50	0.419	2.80	2.65×10^{-9}
55	0.49	1.970	2.85	1.50×10^{-10}

order to evaluate the fitting of the kinetic model, Chi-square (χ^2) tests were done according to Eq. (5) [15]:

$$\chi^2 = \sum \left(\frac{(q_t - q_m)^2}{q_m} \right) \quad (5)$$

where q_t and q_m are the HCl interaction capacities (mol g⁻¹) calculated using experimental data and an specific kinetic model, respectively. The Chi-square statistic test is basically the sum of the squares of the differences between the experimental data and theoretically predicted data from models. If modeled data are similar to the experimental data, χ^2 will be a small number; if they are different, χ^2 will be a large number [21]. The kinetic parameters, presented in Table 1, have excellent agreements of the experimental and calculated data (χ^2 less than 3.00×10^{-9}). The numerical values of the n and k parameters are different in relation to temperature. In this manner, the adsorption kinetic parameters seem to present temperature dependence.

The mechanistic interpretation of the kinetic constant n is difficult and open to interpretation. In general, the values of n from 0.5 to about 1.5 have been related to surface reactions and from 3.0 to about 4.0 to three-dimensional interactions at solid/solution interfaces. When interaction occurs on specific sites, interactions may be random leading to high values for n (2, 3 or higher). In last stages of equilibrium, the interaction may be restricted to one or two dimensions. So, saturation may lead to n values of 1, 2 or 3 for surface, edge and point sites in internal sites of the adsorbent, respectively [42]. The results of the kinetic modeling suggest that surface reactions constitute the majority of the interactions at epoxy/chitosan-modified cement slurry/HCl interface.

Mechanisms involved at solid/solution interfaces can include chemisorption, complexation, ion exchange and adsorption-complexation on surface. An interaction process at solid/solution interfaces can be described by the following consecutive steps (i) transport of solute in the bulk of the solution; (ii) diffusion of solute across the so-called liquid film surrounding sorbent particles; (iii) diffusion of solute in the liquid contained in the pores of sorbate particle and along the pore walls (intraparticle diffusion); (iv) adsorption and desorption of solute molecules on/from the sorbent surface. The overall sorption rate may mainly be controlled by any of these steps; a combined effect of a few steps is also possible [15,42,43].

When in series, these steps are coupled in the sense that the products of one step are the reactants of the next step, and so on. Often, one step has a significantly lower rate than any of the other steps in the sequence. In that case, all but the slowest step, the rate controlling step, can reach the equilibrium conditions [42]. In this simple case where one step is rate-controlling, that step alone is responsible for the observed kinetic rate equation, the rate constant, and their temperature dependences. When the rates of two or more fundamental steps are comparable, then the rate equations and their dependence on system variables can be significantly more complicated and difficult to determine using mathematical modeling.

Taking into account that step (iv) makes a significant contribution in the kinetics of a process, this step is referred to as “surface reaction”. The “surface reaction” term may mean that the actual chemical reaction occurring on the slurry surface involves the formation of chemical bonds. The crucial assumption behind this model is that the rate of the transfer of solute molecules from the solution (located in the direct vicinity of the surface) to the adsorbed phase either governs the overall rate of sorption process or at least is partially involved in it. During the initial stage of acid adsorption, film diffusion may be rate-controlling because large external site bearing surface areas are available. However, with increasing time the external surface layers become saturated

and the rate-controlling step moves to either the speed of reaction at a site (reaction kinetic control) or to internal diffusion, either by pore, surface, or both [43].

In order to confirm more details of the interaction mechanisms of the Chit/epoxy-slurry cement slurry, additional experiments will be carried out using other experimental parameters.

4. Conclusions

In this study, a new epoxy/chitosan-modified cement slurry was synthesized. The features of the new slurry were evaluated in relation to a standard cement slurry ($w/c=0.5$). Characterization has suggested that the new slurry has lower amounts of portlandite in relation to the standard cement slurry. The crystalline pattern of the new slurry was preserved after HCl interaction. On the other hand, the standard slurry, which presents a similar composition in relation to the common cement slurry used in routine operations of oil well cementation, has presented profound modifications after contact with the same HCl solution. It is noted that the interaction of the standard slurry with HCl decreased drastically its crystallinity features. The kinetic data of the interaction of the new slurry with acidic species of HCl in solution were well fitted to an Avrami-like three-parameter kinetic model. The analysis of the kinetic modeling suggests that surface reactions constitute the main interactions at the interface of epoxy/chitosan-modified cement slurry/HCl.

Evidently, additional API standard testing procedures must also be performed in order to use the new cement slurry in long term oil well cementing operations. However, the results of both the characterization of the slurries and the kinetic modeling of HCl interaction underline the excellent features of the epoxy/chitosan-modified cement slurry for using in environmental-friendly acidizing procedures of oil wells.

Acknowledgements

The authors are indebted to the Brazilian agencies CAPES and CNPq for financial support and fellowships.

References

- [1] P.C. Hewlett (Ed.), *Lea's Chemistry of Cement and Concrete*, Elsevier, Burlington, 1998.
- [2] G. Le Saout, E. Lecolier, A. Rivereau, H. Zanni, Chemical structure of cement aged at normal and elevated temperatures and pressures. Part II. Low permeability class G oil well cement, *Cem. Concr. Res.* 36 (2006) 428–433.
- [3] S. Portier, F.-D. Vuataz, P. Nami, B. Sanjuan, A. Gerard, Chemical stimulation techniques for geothermal wells: experiments on the three-well EGS system at Soultz-sous-Forêts, France, *Geothermics* 38 (2009) 349–359.
- [4] H.W. Dorner, R.E. Beddoe, Prognosis of concrete corrosion due to acid attack, in: 9th International Conference of Building Materials, Brisbane, Australia, 2002.
- [5] D.A. Silva, P.J.M. Monteiro, Hydration evolution of C3S–EVA composites analyzed by soft X-ray microscopy, *Cem. Concr. Res.* 35 (2005) 351–357.
- [6] J.J. Chen, D. Zampini, A. Walliser, High-pressure epoxy-impregnated cementitious materials for microstructure characterization, *Cem. Concr. Res.* 32 (2002) 1–7; F. Djouani, C. Connan, M.M. Chehimi, K. Benzarti, Interfacial chemistry of epoxy adhesives on hydrated cement paste, *Surf. Interface Anal.* 40 (2008) 146–150.
- [7] R. Mezzenga, L. Boogh, J.-A.E. Manson, A review of dendritic hyperbranched polymer as modifiers in epoxy composites, *Compos. Sci. Technol.* 61 (2001) 787–795.
- [8] V.L. Zvetkov, R.K. Krastev, V.I. Samichkov, Rate equations in the study of the DSC kinetics of epoxy-amine reactions in an excess of epoxy, *Thermochim. Acta* 478 (2008) 17–27.
- [9] R. Ruehl, Epoxy resins – the current topic on hazardous material, *Gefahrst. Reinhalt. Luft.* 70 (2010) 1.
- [10] J. Williams, R. Nixon, *Brit. J. Dermat.* 159 (2008) 80–81.
- [11] E.M. Petrie, *Epoxy Adhesives Formulations*, Mc-Graw-Hill, New York, 2006.
- [12] E. Guibal, Interactions of metal ions with chitosan-based sorbents: a review, *Sep. Purif. Technol.* 38 (2004) 43–74.
- [13] A.R. Cestari, E.F.S. Vieira, J.A. Mota, The removal of an anionic red dye from aqueous solutions using chitosan beads – the role of experimental factors on adsorption using a full factorial design, *J. Hazard. Mater.* 160 (2008) 337–343.
- [14] A.R. Cestari, E.F.S. Vieira, F.C. da Rocha, Kinetics of interaction of hardened oil-well cement slurries with acidic solutions from isothermal heat-conduction calorimetry, *Thermochim. Acta* 430 (2005) 211–215.
- [15] A.R. Cestari, E.F.S. Vieira, A.M.G. Tavares, M.A.S. Andrade Jr., Cement-epoxy/water interfaces – energetic, thermodynamic, and kinetic parameters by means of heat-conduction microcalorimetry, *J. Colloid Interface Sci.* 343 (2010) 162–167.
- [16] W. Nocuń-Wczelik, Z. Konik, A. Stok, Blended systems with calcium aluminate and calcium sulphate expansive additives, *Constr. Build. Mater.* 25 (2011) 939–943.
- [17] R.E. Beddoe, H.W. Dorner, Modelling acid attack on concrete. Part I. The essential mechanisms, *Cem. Concr. Res.* 35 (2005) 2333–2339.
- [18] V. Ershadi, T. Ebadi, A.R. Rabani, L. Ershadi, H. Soltanian, The effect of nanosilica on cement matrix permeability in oil well to decrease the pollution of receptive environment, *Int. J. Environ. Sci. Develop.* 2 (2011) 128–132.
- [19] J.F. Young, Effect of organic compounds on the interconversion of calcium aluminate hydrates: hydration of monocalcium aluminate, *Cem. Concr. Res.* 1 (1971) 113–122.
- [20] A. Popova, G. Geoffroy, Interactions between polymeric dispersants and calcium silicate hydrates, *J. Am. Ceram. Soc.* 83 (2000) 2556–2560.
- [21] M. Dasha, F. Chiellini, R.M. Ottenbrite, E. Chiellini, Chitosan – a versatile semi-synthetic polymer in biomedical applications, *Prog. Polym. Sci.* 36 (2011) 981–1014.
- [22] R. Mezzenga, L. Boogh, J.-A.E. Manson, A review of dendritic hyperbranched polymer as modifiers in epoxy composites, *Compos. Sci. Technol.* 61 (2001) 787–795.
- [23] A. Hidalgo, C. Domingo, C. Garcia, S. Petit, C. Andrade, C. Alonso, Microstructural changes induced in Portland cement-based materials due to natural and supercritical carbonation, *J. Mater. Sci.* 43 (2008) 3101–3111.
- [24] J. Björnström, A. Martinelli, A. Matic, L. Börjesson, I. Panas, Accelerating effects of colloidal nano-silica for beneficial calcium–silicate–hydrate formation in cement, *Chem. Phys. Lett.* 392 (2004) 242–248.
- [25] I. García-Lodeiro, A. Fernández-Jiménez, M. Teresa Blanco, A. Palomo, FTIR study of the sol–gel synthesis of cementitious gels: C–S–H and N–A–S–H, *J. Sol–Gel Sci. Technol.* 45 (2008) 63–72.
- [26] A. Jennia, L. Holzerb, R. Zurbriggenc, M. Herwegh, Influence of polymers on microstructure and adhesive strength of cementitious tile adhesive mortars, *Cem. Concr. Res.* 35 (2005) 35–50.
- [27] F. Djouani, C. Connan, M. Delamar, M.M. Chehimi, K. Benzarti, Cement paste–epoxy adhesive interactions, *Constr. Build. Mater.* 25 (2011) 411–423.
- [28] A.R. Cestari, E.F.S. Vieira, A.A. Pinto, F.C. da Rocha, Synthesis and characterization of epoxy-modified cement slurries – kinetic data at hardened slurries/HCl interfaces, *J. Colloid Interface Sci.* 327 (2008) 267–274.
- [29] G. Le Saout, É. Lécolier, A. Rivereau, H. Zanni, Study of oilwell cements by solid-state NMR, *C. R. Chimie* 7 (2004) 383–388.
- [30] A. Palomo, M.W. Grutzeck, M.T. Blanco, Alkali-activated fly ashes: a cement for the future, *Cem. Concr. Res.* 29 (1999) 1323–1329.
- [31] A. Chaipanich, T. Nochaiya, Thermal analysis and microstructure of Portland cement-fly ash-silica fume pastes, *J. Therm. Anal. Calorim.* 99 (2010) 487–493.
- [32] L. Alarcon-Ruiza, G. Platretb, E. Massieub, A. Ehrlacher, The use of thermal analysis in assessing the effect of temperature on a cement paste, *Cem. Concr. Res.* 35 (2005) 609–613.
- [33] S.M. Antao, M.J. Duane, I. Hassan, DTA, TG, and XRD studies of sturmanite and ettringite, *Canad. Mineral.* 40 (2002) 1403–1409.
- [34] E.F.S. Vieira, A.R. Cestari, R.G. da Silva, A.A. Pinto, C.R. Miranda, A.C.F. Conceição, Use of calorimetry to evaluate cement slurry resistance to the attack of acid solutions, *Thermochim. Acta* 419 (2004) 45–49.
- [35] R. Ylména, L. Wadsö, I. Panas, Insights into early hydration of Portland limestone cement from infrared spectroscopy and isothermal calorimetry, *Cem. Concr. Res.* 40 (2010) 1541–1546.
- [36] T. Nagano, S. Nakashima, S. Nakayama, K. Osada, M. Senoo, *Clays Clay Miner.* 40 (1992) 600–607.
- [37] J. Torrent, V. Barrón, Diffuse reflectance spectroscopy of iron oxides, in: *Encyclopedia of Surface and Colloid Science*, Marcel Dekker, New York, 2002.
- [38] D.C. MacLaren, M.A. White, Cement: its chemistry and properties, *J. Chem. Educ.* 80 (2003) 623–635.
- [39] A. Allahverdi, F. Škvára, Acidic corrosion of hydrated cement based materials. Part 2. Kinetics of the phenomenon and mathematical models, *Ceramics – Silikáty* 44 (2000) 152–160.
- [40] A.R. Cestari, E.F.S. Vieira, A.J.P. Nascimento, New factorial designs to evaluate chemisorption of divalent metals on aminated silicas, *J. Colloid Interface Sci.* 241 (2001) 45–51.
- [41] A.R. Cestari, E.F.S. Vieira, J.D.S. Matos, Determination of kinetic parameters of Cu(II) interaction with chemically modified thin chitosan membranes, *J. Colloid Interface Sci.* 285 (2005) 288–295.
- [42] K.O. Moura, E.F.S. Vieira, A.R. Cestari, The use of solution microcalorimetry to evaluate chemically modified fish scales as a viable adsorbent for heavy metals, *J. Therm. Anal. Calorim.*, doi:10.1007/s10973-011-1612-8, in press.
- [43] W. Plazinski, W. Rudzinski, A. Plazinska, Theoretical models of sorption kinetics including a surface reaction mechanism: a review, *Adv. Colloid Interface Sci.* 152 (2009) 2–13.